Metabolic control of G1–S transition: cyclin E degradation by p53-induced activation of the ubiquitin–proteasome system

Sudip Mandal,[1] William A. Freije,[2] Preeta Guptan,[4] and Utpal Banerjee[1,3]

[1]Department of Molecular, Cell, and Developmental Biology, Molecular Biology Institute, [2]Department of Obstetrics and Gynecology, David Geffen School of Medicine, and [3]Department of Biological Chemistry, University of California, Los Angeles, Los Angeles, CA 90095
[4]Wisconsin Alumni Research Foundation, University of Wisconsin, Madison, WI 53726

Cell cycle progression is precisely regulated by diverse extrinsic and intrinsic cellular factors. Previous genetic analysis in *Drosophila melanogaster* has shown that disruption of the mitochondrial electron transport chain activates a G1–S checkpoint as a result of a control of cyclin E by p53. This regulation does not involve activation of the p27 homologue dacapo in flies. We demonstrate that regulation of cyclin E is not at the level of transcription or translation. Rather, attenuated mitochondrial activity leads to transcriptional upregulation of the F-box protein archipelago, the Fbxw7 homologue in flies. We establish that archipelago and the proteasomal machinery contribute to degradation of cyclin E in response to mitochondrial dysfunction. Our work provides in vivo genetic evidence for p53-mediated integration of metabolic stress signals, which modulate the activity of the ubiquitin–proteasome system to degrade cyclin E protein and thereby impose cell cycle arrest.

Introduction

Molecular genetic analysis in *Drosophila melanogaster* has revealed that G1–S transition in mitosis can be modulated by the metabolic status of the cell (Mandal et al., 2005; Owusu-Ansah et al., 2008). Cells harboring a mutation in the gene encoding cytochrome C oxidase subunit Va (CoVa) of complex IV of the electron transport chain display a reduced level of cellular ATP and a consequent increase in the levels of cellular AMP. A signaling pathway that involves AMPK and p53 is then activated to reduce cyclin E protein level and cause G1–S arrest (Mandal et al., 2005). Unlike the results obtained in mammalian systems upon DNA damage induced by γ-irradiation (el-Deiry et al., 1993; Levine, 1997), this p53-mediated cyclin E effect in flies is not a consequence of Cdk inhibitor up-regulation, as the expression of dacapo, the p27 homologue in flies (de Nooij et al., 1996; Lane et al., 1996), is not affected in *CoVa* mutant cells (Mandal et al., 2005). The mechanism by which p53 controls cyclin E protein under conditions of metabolic stress was not well understood and forms the central focus of this study.

Progression from G1 to S phase of cell cycle is primarily regulated by the activity of the cyclin E–Cdk2 complex (Hwang and Clurman, 2005). An intricate balance between its timed synthesis and rapid degradation by the ubiquitin–proteasome system maintains the oscillating level of cyclin E during the cell cycle and ensures unidirectional and irreversible transition of a cell through the G1–S checkpoint (Reed, 2003). Processing by the ubiquitin–proteasome system involves the covalent attachment of ubiquitin molecules to the target protein followed by its degradation by the proteasome (Hershko, 2005). In flies, as well as in mammals, the ubiquitinylation of cyclin E is mediated by the Skp1–Cul1–F-box protein (SCF) complex (Nakayama and Nakayama, 2006). During normal cell cycle progression in mammals, recruitment of cyclin E to the SCF complex can be achieved by either of the two F-box proteins Fbxw7 or Skp2 (Nakayama et al., 2000; Koepp et al., 2001; Strohmaier et al., 2001), whereas in flies, only the Fbxw7

The Rockefeller University Press $30.00
J. Cell Biol. Vol. 188 No. 4   473–479
www.jcb.org/cgi/doi/10.1083/jcb.200912024

JCB   473

homologue archipelago is involved in this process (Moberg et al., 2001). Further studies revealed the existence of a second cyclin E degradation mechanism involving Cullin 3, which occurs in an SCF-independent manner (Singer et al., 1999; Wimuttisuk and Singer, 2007). Together, these pathways are instrumental in achieving a rapid turnover of cyclin E during early S phase of the normal cell cycle.

In human and murine systems, p53 acts as a cellular hub for integrating diverse stress signals to generate different cellular responses that range from a block in cell cycle progression to the induction of apoptosis (Vousden and Lane, 2007; Jones and Thompson, 2009). In flies, the role of p53 has mainly been studied with relation to radiation-induced damage (Brodsky et al., 2000; Sogame et al., 2003). Based on those findings, coupled with the fact that there is no identified p21 homologue in flies and that *dacapo* (*p27*) is not responsive to irradiation (de Nooij et al., 1996), it was believed that in *Drosophila*, the p53 response to stress is primarily restricted to the activation of apoptosis and does not involve cell cycle control. However, our previous experiments indicated a role for p53 in promoting G1–S arrest in response to mitochondrial dysfunction (Mandal et al., 2005).

The following results unravel the mechanistic basis for this p53-induced G1–S block under conditions of attenuated mitochondrial function. Based on in vivo genetic analysis as well as in vitro studies involving *CoVa* mutants, we demonstrate that the activation of p53 under conditions of metabolic stress causes transcriptional up-regulation of the F-box protein archipelago. We establish a role for archipelago and the proteasomal machinery in the degradation of the cyclin E protein during mitochondrial dysfunction.

Results and discussion

The developing eye disc of *Drosophila* has been extensively used as a genetic model to understand mechanisms of intercellular signaling, pattern formation, and cell cycle control (Edgar and Lehner, 1996; Baker, 2001; Nagaraj and Banerjee, 2004). During the third larval instar, patterning of the retinal epithelium begins at the posterior end of the eye disc and progresses as a wave toward the anterior (Wolff and Ready, 1991). An indentation termed the morphogenetic furrow (MF) marks the leading edge of this wave (Fig. 1 A). Cells anterior to the furrow divide asynchronously but are arrested in the G1 phase at the MF. As the furrow progresses, a subset of these cells synchronously enters the S phase of a terminal round of cell division commonly termed the second mitotic wave (SMW; Fig. 1 A). These two distinct phases of cell division become apparent upon BrdU incorporation, a process that specifically marks cells in S phase (Fig. 1 B). This stereotyped pattern of incorporation is disrupted in eye discs bearing clones of *CoVa* mutations as the mutant tissue, either anterior or posterior to the MF, fail to incorporate BrdU (Fig. 1, compare B with C). However, a significant recovery in BrdU incorporation occurs in clones that are mutant for both *CoVa* and *p53* (Fig. 1 D), suggesting that p53 functions downstream of *CoVa* in the pathway that is involved in the mitotic checkpoint control (Mandal et al., 2005).

Consistent with the synchronous entry of wild-type cells into S phase posterior to the MF, cyclin E is expressed in a narrow stripe of cells immediately posterior to the furrow (Fig. 1 E; Richardson et al., 1995). This expression of cyclin E is significantly reduced in *CoVa* clones (Fig. 1 F) but can be restored to normal levels if the cells are also mutant for *p53* (Fig. 1 G). Loss of cyclin E in *CoVa* mutant cells is not at the level of transcription because wild-type amounts of *cyclin E* transcripts are expressed in *CoVa*-null mutant clones and in S2 cells in which CoVa is knocked down by RNAi (Fig. 1 L; Mandal et al., 2005). Consequently, in this study, we sought to describe a posttranscriptional mechanism that could account for the loss of cyclin E protein in *CoVa* mutant cells.

For a vast majority of known examples, regulation at the level of mRNA translation is achieved through the interaction of factors with untranslated sequences (5′ and 3′ untranslated regions [UTRs]) of the mRNA (de Moor et al., 2005; Pickering and Willis, 2005). We cloned the 5′ and 3′ UTRs of *cyclin E* mRNA and placed them upstream and downstream, respectively, of a reporter GFP coding sequence and expressed it in S2 cells under the control of an inducible *metallothionein* promoter (Fig. 1 H). These cells were transfected with either *CoVa* double-stranded RNA (dsRNA) or *GST* dsRNA (as control). No change in GFP expression was detected in *CoVa* dsRNA–treated cells compared with the control (Fig. 1, I–L). However, the CoVa-depleted cells showed a clear reduction in the level of endogenous cyclin E protein (Fig. 1 L). Consistent with earlier results, the expression of cyclin E transcript remains unchanged in *CoVa* dsRNA–treated cells (Fig. 1 M). These results reiterate that the control of cyclin E in the context of mitochondrial dysfunction is posttranscriptional, and based on these results, we consider it unlikely that the UTRs of the cyclin E transcript are involved in this regulation.

To investigate whether the loss of cyclin E protein in the *CoVa* mutants resulted from its proteasomal degradation, we used a mutation in the gene *l(3)73Ai*, which encodes the β6 subunit of the 20S proteasome core complex (Saville and Belote, 1993). One copy loss of *l(3)73Ai* suppresses the *CoVa* mutant phenotype and causes the restoration of the normal pattern of BrdU incorporation (Fig. 1 N) and cyclin E expression (Fig. 1 O) in *CoVa* mutant clones. Interestingly, the glossy adult eye phenotype of *CoVa* mutant clones (Fig. 1, P–Q′, marked by the absence of red pigmentation) is also significantly suppressed (Fig. 1, R and R′). These results establish that cyclin E proteins can be restored to sufficiently high levels, allowing *CoVa* mutant cells to overcome the G1–S block upon attenuation of proteasomal function.

To further investigate a possible role for the ubiquitin–proteasome degradation pathway in the loss of cyclin E, we analyzed the genetic interaction between *CoVa* and genes that encode members of the SCF complex. One copy loss of *archipelago* (*ago*) could significantly suppress the BrdU defect in *CoVa* mutant clones (Fig. 2 A) and restore the normal expression of cyclin E (Fig. 2 B). A significant suppression of the *CoVa* adult eye phenotype was also seen in a genetic background that is heterozygous for *ago* (Fig. 2, C and C′) in addition to being *CoVa⁻/CoVa⁻*. In contrast, loss of one copy of
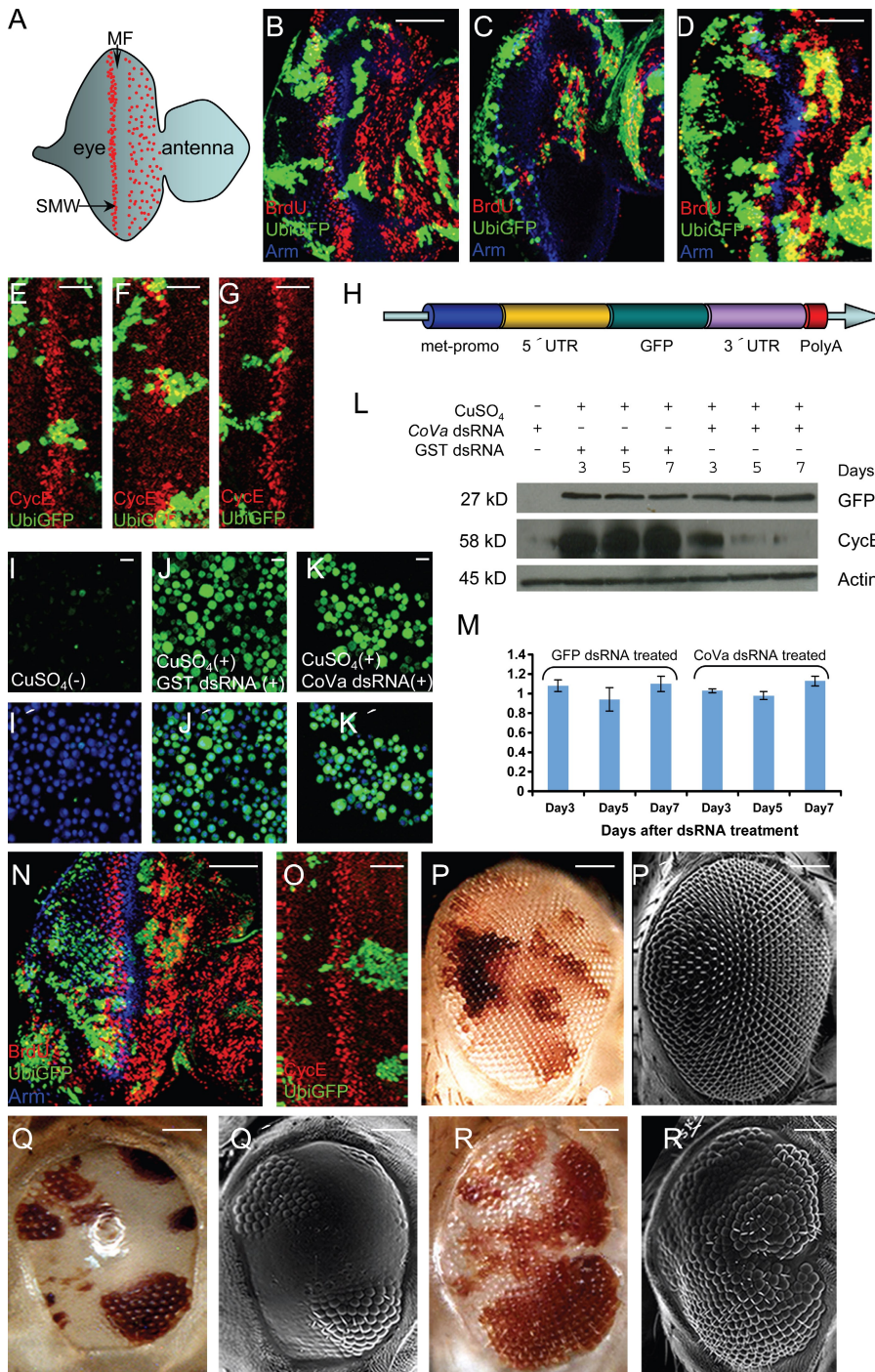
Figure 1. Regulation of cyclin E in *CoVa* mutant cells. (A) Schematic diagram of a developing third instar larval eye disc of *Drosophila*. Anterior is to the right. Scattered red dots anterior to the MF represent random BrdU incorporation, whereas the band of red dots marks the synchronous incorporation of BrdU along the SMW. (B–D) The defect in BrdU incorporation in *CoVa* mutants can be rescued by *p53* mutation. BrdU incorporation (red) in third instar larval eye disc. Armadillo (blue) marks the MF, and the clones are marked by the lack of GFP. Bars, 50 µm. (B) The normal pattern of BrdU incorporation in a control eye disc in which both green and nongreen cells are wild type. (C) An eye disc with somatic clones of *CoVa⁻/CoVa⁻* cells (nongreen) fails to incorporate BrdU both anterior and posterior to the MF. (D) Somatic clones of *CoVa⁻/CoVa⁻*, *p53⁻/p53⁻* cells (nongreen) are rescued for BrdU incorporation (compare with C). (E–G) *p53* mutation restores cyclin E expression (red) along the SMW in *CoVa* mutant clones. Clones are marked by the absence of GFP. Bars, 25 µm. (E) Expression of cyclin E as a band posterior to the furrow in a control eye disc where both the green and the nongreen cells are wild type. (F) Cyclin E expression is significantly reduced in *CoVa* mutant clones (nongreen). (G) In double-mutant clones of *CoVa* and *p53* (nongreen), cyclin E expression recovers to wild-type levels. (H) A reporter construct used to investigate possible roles of cyclin E 5′ and 3′ UTRs in translational regulation. This construct consists of a GFP-expressing fragment cloned between the 5′ and 3′ UTRs of cyclin E. The expression of GFP transcripts is under the control of a *metallothionein*-inducible promoter. (I–K′) CuSO₄-inducible GFP expression is not affected in S2 cells harboring the 5′-3′ cyclin E UTR-GFP reporter upon *CoVa* dsRNA treatment. In I–K, the GFP expression is shown in green, and the overlap of GFP expression with the cell nuclei marked by TO-PRO 3 (blue) is shown in I′–K′. Bars, 20 µm. (I and I′) Very low levels of basal GFP expression in cells that are not induced by CuSO₄. (J and J′) Reporter GFP expression in control cells that are transfected with *GST* dsRNA. (K and K′) Compared with control, no change in reporter GFP expression is seen in cells transfected with *CoVa* dsRNA. (L) Western blot analysis performed 3, 5, and 7 d after treatment of S2 cells with *GST* dsRNA or *CoVa* dsRNA by using the indicated antibodies. Levels of GFP reporter expression are comparable in both *GST* and *CoVa* dsRNA–treated cells, but cyclin E expression is dramatically reduced in *CoVa* dsRNA–transfected cells. Actin was used as a loading control, and the lanes are as indicated. (M) Real-time RT-PCR analysis of cyclin E transcripts in S2 cells on 3, 5, or 7 d after treatment with either *GST* or *CoVa* dsRNA. Unlike the loss of cyclin E protein seen in L, cyclin E RNA levels remain unchanged. The data were normalized with respect to the expression of rp49 transcripts. (N) BrdU incorporation (red) in eye disc with clones of *l(3)73Ai⁻/ l(3)73Ai⁺*, *CoVa⁻/CoVa⁻* cells (nongreen). A remarkable recovery of BrdU incorporation is seen in these clones (compare with C). *l(3)73Ai* encodes the β6 subunit of 20S proteasome core. Bar, 50 µm. (O) Expression of cyclin E (red) is also restored to wild-type levels in clones with *l(3)73Ai⁻/ l(3)73Ai⁺*, *CoVa⁻/CoVa⁻* cells (nongreen; compare with F). Bar, 25 µm. (P–R′) Reduced dosage of *l(3)73Ai* partially rescues the glossy adult eye phenotype of *CoVa* mutant clones. Bright-field images (P–R) and the corresponding scanning electron micrographs (P′–R′) of the same adult eye with somatic clones (marked by the absence of red pigmentation). (P and P′) Normal facets in control adult eye in which both red and white tissue are wild type. (Q and Q′) Adult eye with clones of *CoVa⁻/CoVa⁻* cells. Facets are identifiable in the wild-type tissue (red), whereas the mutant tissue (white) appears glossy. (R and R′) The glossy eye phenotype of *CoVa* clones is partially rescued in clones of *l(3)73Ai⁻/ l(3)73Ai⁺*, *CoVa⁻/CoVa⁻* cells. Bars, 100 µm. Error bars indicate SEM.

Cullin 1 or *Cullin 3*, other potential members responsible for ubiquitinylation of cyclin E, did not rescue the defects in BrdU incorporation (Fig. 2, D and E) in *CoVa* mutant clones. These dosage-sensitive interactions with *ago* suggest that the archipelago protein functions upstream of cyclin E and is therefore a potential target for p53. Consistent with this observation,

Figure 2. Loss of *ago* rescues the *CoVa* mutant phenotype. (A) Defects in BrdU incorporation (red) is significantly recovered in eye disc with clones of *ago*⁺/*ago*⁻, *CoVa*⁻/*CoVa*⁻ cells (nongreen; compare with Fig. 1 C). Armadillo (blue) marks the MF. Bar, 50 µm. (B) Loss of *ago* restores wild-type expression of cyclin E (red) along the SMW in eye discs with clones of *ago*⁺/*ago*⁻, *CoVa*⁻/*CoVa*⁻ cells (nongreen; compare with Fig. 1 F). Bar, 25 µm. (C and C′) Bright-field image (C) and the corresponding SEM (C′) of an adult eye with clones of *ago*⁺/ *ago*⁻, *CoVa*⁻/*CoVa*⁻ cells. Mutant clones are marked by the absence of red pigmentation. Loss of *ago* partially rescues the glossy adult eye phenotype associated with *CoVa* mutant clones (compare with Fig. 1, R and R′). Bars, 100 µm. (D and E) Reducing the dosage of *Cullin* 1 (D) or *Cullin* 3 (E) in *CoVa* mutant cells (nongreen) fails to rescue the defects in BrdU incorporation (red). Bars, 50 µm. (F) Expression profile of *ago* in S2 cells treated with *CoVa* dsRNA or GFP dsRNA controls. Gene expression profiling was performed in three independent replicates (Exp. 1–3) using *Dro-sophila* genome 2 microarrays. The guide at the bottom of the figure indicates the fold difference of expression between the samples, with green indicating lower expression and red indicating higher expression. (G) Real-time RT-PCR analysis of *ago* transcripts in S2 cells treated either with *CoVa* dsRNA or GFP dsRNA (control) that were used for performing the microarray analysis. An up-regulation in *ago* expression is observed in cells knocked down for *CoVa* transcripts compared with the control. Error bars indicate SEM.
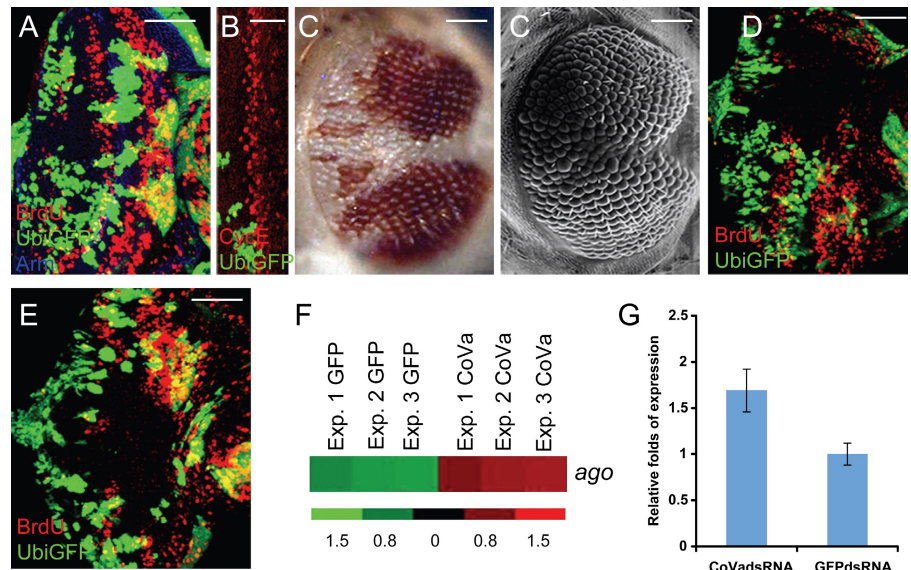
our experiments of differential gene expression profiling using microarrays showed an increase in the level of *ago* expression in S2 cells expressing RNAi for *CoVa* compared with those expressing GFP RNAi as control (Fig. 2 F). This up-regulation in *ago* expression in *CoVa*-depleted S2 cells was subsequently validated by real-time RT-PCR (Fig. 2 G).

As an in vivo correlate of this result, we observed that even in eye discs having clones of *CoVa* mutant cells, *ago* is expressed at a higher level compared with those discs having clones of wild-type cells (Fig. 3 A). Interestingly, this up-regulation in *ago* expression is dependent on *p53*, as its expression is restored to normal levels in eye discs having clones that are double mutant for CoVa and p53 (Fig. 3 A). Together, these results clearly establish that up-regulation of *ago* induced by metabolic stress in *CoVa* mutant cells is mediated by p53. To determine whether this up-regulation of *ago* is directly controlled by p53, we initiated a biochemical approach. The p53 protein functions as a sequence-specific DNA-binding factor and can activate genes whose promoters contain a p53 response element (el-Deiry et al., 1992; Farmer et al., 1992). Within 100 bp upstream of the transcriptional initiation site of *ago*, we identified a 21-bp sequence (Fig. 3 B) that strongly resembles the consensus for the p53 DNA-binding site (el-Deiry et al., 1992). Like those found upstream of the human target genes *mdm-2* (Wu et al., 1993) and *p21/WAF1* (el-Deiry et al., 1993) or that of *Drosophila* apoptotic gene *reaper* (Brodsky et al., 2000), this putative p53-binding site upstream of *ago* contains two tandemly arrayed 10 mers separated by a single nucleotide spacer (Fig. 3 C). The putative p53-binding site upstream of *ago* is highly conserved among the members of the *melanogaster* subgroup of *Drosophila* that diverged over 10 million years ago (Fig. 3 D). Binding of p53 to this response element was investigated by EMSA. As shown in Fig. 3 E, p53 binds to the potential binding sequence, and this binding can be efficiently

competed with unlabeled oligonucleotides or eliminated when the binding sequence is mutated. To find a functional correlate, we cloned the archipelago promoter having either a normal or mutated p53-binding site upstream of the firefly luciferase reporter gene (Fig. 3 F) and transfected S2 cells. We observed that upon knocking down CoVa while cells with a normal p53-binding site in *ago* promoter lead to an increase in firefly luciferase expression, cells with a mutated p53-binding site in *ago* promoter showed luciferase expression comparable with control cells. S2 cells having normal *ago* promoter upstream of luciferase treated with GFP dsRNA were used as controls (Fig. 3 G). These results strongly suggest that *ago* can function as a direct downstream target of p53.

A schematic of the signaling pathway linking attenuated mitochondrial function to proteasomal degradation of cyclin E unraveled primarily based on loss of function genetic analysis is shown in Fig. 3 H. We conclude that AMP is used as a metabolic signal for distressed mitochondrial function to initiate a cascade that involves activation of AMPK and p53 (Mandal et al., 2005) followed by the transcriptional up-regulation of *ago*. This leads to ubiquitinylation of cyclin E by the SCF complex and its subsequent degradation by the proteasome. As a consequence, cell cycle progression is blocked at the G1–S transition. Such mitochondrially regulated checkpoints could be useful for a temporary arrest in the cell cycle to tide over conditions of energy deficiency or hypoxia. By initiating a G1–S checkpoint, a cell lacking in adequate ATP levels ensures that it is not irreversibly damaged during the S phase but can resume proliferation upon restoration of normal conditions.

Studies in mouse and human cell lines have demonstrated that the expression of *CDC4b*, the gene that encodes the Fbxw7β isoform, is dependent on irradiation-induced p53 activation and have implicated this protein in p53-mediated cell cycle arrest as a result of radiation damage (Kimura et al., 2003; Mao et al., 2004;
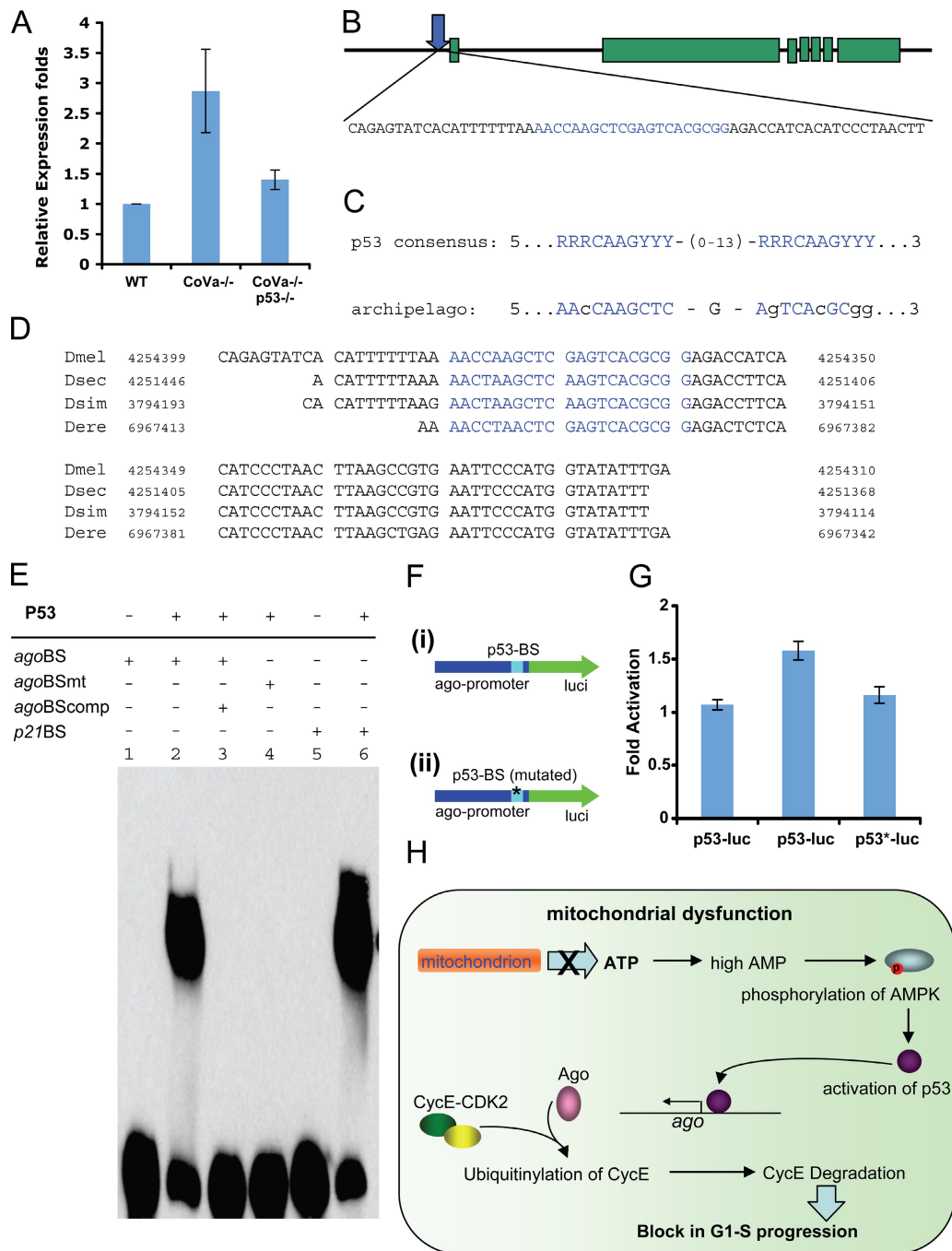
A

Relative Expression folds

WT CoVa-/- CoVa-/- p53-/-

B

CAGAGTATCACATTTTTTAAAACCAAGCTCGAGTCACGCGGAGACCATCACATCCCTAACTT

C

```
p53 consensus:  5...RRRCAAGYYY-(0-13)-RRRCAAGYYY...3

archipelago:    5...AAcCAAGCTC - G - AgTCAcGCgg...3
```

D

```
Dmel  4254399  CAGAGTATCA CATTTTTTAA AACCAAGCTC GAGTCACGCG GAGACCATCA  4254350
Dsec  4251446           A CATTTTTAAA AACTAAGCTC AAGTCACGCG GAGACCTTCA  4251406
Dsim  3794193          CA CATTTTTAAG AACTAAGCTC AAGTCACGCG GAGACCTTCA  3794151
Dere  6967413          AA AACCTAACTC GAGTCACGCG GAGACTCTCA             6967382

Dmel  4254349  CATCCCTAAC TTAAGCCGTG AATTCCCATG GTATATTTGA             4254310
Dsec  4251405  CATCCCTAAC TTAAGCCGTG AATTCCCATG GTATATTT                4251368
Dsim  3794152  CATCCCTAAC TTAAGCCGTG AATTCCCATG GTATATTT                3794114
Dere  6967381  CATCCCTAAC TTAAGCTGAG AATTCCCATG GTATATTTGA             6967342
```

E

P53	−	+	+	+	−	+
*ago*BS	+	+	+	−	−	−
*ago*BSmt	−	−	−	+	−	−
*ago*BScomp	−	−	+	−	−	−
*p21*BS	−	−	−	−	+	+
	1	2	3	4	5	6

F

(i) p53-BS
ago-promoter   luci

(ii) p53-BS (mutated) *
ago-promoter   luci

G

Fold Activation

p53-luc   p53-luc   p53*-luc

H

mitochondrial dysfunction

mitochondrion X→ ATP → high AMP → phosphorylation of AMPK

Ago

CycE-CDK2 → activation of p53 → *ago*

Ubiquitinylation of CycE → CycE Degradation

Block in G1-S progression

Figure 3. ***ago* is a direct downstream target of p53.** (A) Real-time RT-PCR analysis of *ago* transcripts in third instar larval eye discs having somatic clones of wild-type cells, *CoVa* mutant cells (*CoVa*$^{-/-}$), or that of *CoVa* and *p53* double-mutant cells (*CoVa*$^{-/-}$, *p53*$^{-/-}$). The up-regulation in *ago* transcripts as seen in eye discs with *CoVa* mutant cells is restored to almost wild-type level in eye discs with double-mutant clones of *CoVa* and *p53*. (B) Genomic structure of *ago* highlighting the p53 response element in the 5′ regulatory region of *ago-RB* and *ago-RC* transcripts that share the same promoter region. Blue text denotes the putative p53-binding sequence and the mRNA, *ago-RC*, is shown in the figure. (C) Alignment of the consensus p53-binding sequence with the p53 response element found in the 5′ regulatory region of *ago*. The invariant core nucleotides of each 10-mer motif matches at seven of eight positions, whereas the other mismatches (shown in lower case) occur at the outer positions of the 20-bp element. (D) Conserved sequence in the 5′ regulatory region of *ago* across the members of the *melanogaster* subfamily of *Drosophila* with the p53 response element highlighted in blue. (E) EMSA demonstrating the binding of purified p53 to its putative binding sequence in *ago*. (lanes 1 and 2) A shift in the migration of the biotinylated p53 response element of *ago* is seen in the presence of p53 protein. (lane 3) This binding is competed by unlabeled oligonucleotide. (lane 4) Mutating the core nucleotide sequence of the two 10 mers within the p53 response element prevents binding of p53. (lanes 5 and 6) As a control, a shift in the migration of a biotinylated oligonucleotide representing the p53 response element of mammalian *p21* is seen in the presence of p53 protein. (F) The reporter constructs used to investigate p53-dependent activation of *ago* promoter in *CoVa* mutant cells. Construct i consisted of the 200-bp of the *ago* promoter with normal p53-binding site cloned upstream of the firefly luciferase reporter gene. Construct ii is similar to construct i except for the p53-binding site being mutated. (G) Relative folds of activation of the reporter firefly luciferase in *GFP* dsRNA or *CoVa* dsRNA–treated cells. The datasets were normalized to the expression of Renilla luciferase, and mean values with standard deviation of three independent experiments are displayed. Compared with GFP dsRNA–transfected cells, *CoVa* dsRNA–transfected cells show almost 1.7-fold increase in the expression levels of firefly luciferase. However, this increase is not seen when the p53 site in *ago* promoter is mutated. Asterisks indicate a mutation in the P53-binding site (p53BS). (H) A model for the p53-mediated pathway linking attenuated mitochondrial function in *CoVa* mutants to G1–S block caused as a result of degradation of cyclin (E). Error bars indicate SEM.

Perez-Losada et al., 2005; Matsumoto et al., 2006; Minella et al., 2007). In this study, we provide in vivo evidence for a similar pathway used by the cell under conditions of metabolic stress to regulate the levels of cyclin E protein to impose a G1–S block. These results provide an alternate means in *Drosophila* where p53 does not seem to cause p21-mediated cell cycle arrest.

Interestingly, activation of *ago* by p53 is very specific to this pathway, as we do not find any up-regulation of the proapoptotic gene *reaper*, a known downstream target of p53 that is activated upon radiation-induced damage in flies (Brodsky et al., 2000). We deduce that this is possible because the function of p53 in a cell depends on its threshold level. At the p53 activity level maintained in *CoVa* mutants, most cellular functions, such as differentiation and viability continue normally, but a cell cycle checkpoint is specifically activated. Presumably, higher levels of p53 activation would trigger cell death pathway genes as recovery becomes untenable.

Involvement of the ubiquitin–proteasome system in transcriptional regulation of a large number of genes associated with cell cycle progression and apoptosis (Bhaumik and Malik, 2008) has drawn significant attention in recent years to understand the mechanism by which the activity of this system is regulated. Although it is imperative that the metabolic condition of a cell would have a control over the activity of the proteasome system, only a handful of reports have provided insight into the processes by which glucose metabolism can modulate the proteasomal function in flies and mammals (Zhang et al., 2007). From that perspective, this work provides the evidence of an independent mechanism that links the functioning of oxidative phosphorylation to transcriptional regulation of the E3 ligase *ago*. Interestingly, these two mechanisms differ from one another, as they regulate the activity of the ubiquitin–proteasome system at two different levels. Although the cellular glucose level directly regulates the function of the proteasome, the cellular ATP level modulates the process of ubiquitinylation.

Materials and methods

Drosophila stocks and genetics
The following *Drosophila* strains were used: *y, w, ey-flp; FRT82B, CoVa/TM6B, Tb*; and *y, w, ey-flp; FRT82, CoVa, p53/TM6B, Tb* (Mandal et al., 2005); *l(3)73Ai¹/TM6B, Tb* (Saville and Belote, 1993); *ago¹, FRT80B/TM6B, Tb* (Moberg et al., 2001); *cul1^{EX}/Cyo* (Ou et al., 2002); *gft^{HG39}/Cyo* (*Cullin3*; Mistry et al., 2004). Adult eye clones were made by using flies of the genotype *y, w, ey-flp; FRT82B P[w⁺]cl-R3/TM6B Tb, y⁺*. Mutant clones were marked by the absence of pigmentation. Clones in third instar larval eye discs were generated by using flies of the genotype *y, w, ey-flp; FRT82B, Ubi-GFP, RpS3/TM6B Tb, y⁺*, and the clones were marked by the absence of GFP.

Immunohistochemistry
BrdU incorporation in the third instar larval eye imaginal disc was performed as described previously (de Nooij and Hariharan, 1995). In brief, the freshly dissected eye discs were incubated for 30 min in 400 µl 75 µg/ml BrdU in PBS followed by fixation in 4% formaldehyde. The tissues were incubated in primary antibody overnight at 4°C. Incubation in the corresponding secondary antibody was performed for 2 h at room temperature, and the tissues were refixed in formaldehyde for 15 min before DNA denaturation by 2 N HCl. Subsequent incubations in anti-BrdU antibody and the corresponding secondary antibody were performed for overnight at 4°C and for 2 h at room temperature, respectively. The following antibodies were used: rat anti-BrdU (1:100; Abcam), mouse anti–cyclin E (1:50; H. Richardson,

Peter MacCallum Cancer Centre, Melbourne, Victoria, Australia), guinea pig anti–cyclin E (1:150; T. Orr-Weaver, Massachusetts Institute of Technology, Cambridge, MA), mouse anti-GFP and rabbit anti-GFP (1:500; Invitrogen), and mouse anti-Armadillo, (1:250; Iowa Hybridoma Center). CY3, FITC, or CY5-conjugated secondary antibodies (1:400; Jackson ImmunoResearch Laboratories, Inc.) were used. Acquisition of images was performed with a confocal microscope laser-scanning system (Radiance 2000; Bio-Rad Laboratories) and processed with a confocal assistant (Bio-Rad Laboratories).

Cell culture, RNAi, and microarray analysis
To prepare dsRNA, a coding sequence specific to *CoVa*, *GST*, or *GFP* was PCR amplified with primers carrying a 5′ T7 RNA polymerase-binding site. dsRNA was purified by using a Megascript RNAi kit (Ambion). S2 cells were transfected with 20 µg dsRNA as described previously (Clemens et al., 2000). Cells were harvested on 3, 5, and 7 d after transfection for protein analysis. Total RNA was isolated from the cells 7 d after transfection and was used to generate microarray probes that were hybridized to the *Drosophila* genome 2 arrays (Affymetrix). The Gene Chip Operating system (Affymetrix) and dCHIP program (Harvard University) were used to define absent/present calls and to generate pairwise comparisons between the transcription profile of *GFP* and *CoVa* dsRNA–treated S2 cells. The sequences of the primers to generate dsRNAs are provided in Table S1.

EMSA
This assay was performed using the Lightshift chemiluminescent EMSA kit (Thermo Fisher Scientific). Synthetic oligonucleotides containing the putative p53-binding sequence in *ago*, either wild type or mutated for both the core sequences, and the p53-binding sequence in mammalian *p21* were biotinylated at their 5′ ends (IDT). The complementary oligonucleotides were then annealed. The probes were incubated for 20 min at room temperature with 20 ng of purified recombinant p53 protein (Active Motif) in the buffer supplied with the kit. This was followed by electrophoresis in 5% native gels and subsequent transfer onto a nylon membrane. Signals were detected using the standard protocol mentioned in the kit. The sequences of the different oligonucleotides used are provided in Table S2.

Real-time RT-PCR
RNA was extracted using the RNeasy Mini kit (QIAGEN) and reverse transcribed with reverse transcription (Superscript II; Invitrogen). Real-time PCR was performed on the cDNa according to the manufacturer's protocol using iCycler (iQ; Bio-Rad Laboratories) with SYBR green as the fluorophore.

Firefly luciferase reporter assay
The proximal 200 bp up to and including the TATA box of the *ago* promoter having the p53-binding site either normal or mutated were cloned into the pGL3 basic vector containing firefly luciferase (Promega). S2 cells were transfected with either of these reporter constructs in conjunction with dsRNA for GFP (control) or *CoVa* using the calcium phosphate transfection method (Clemens et al., 2000). Transfection also included a luciferase reporter containing a minimal promoter linked to *Renilla* luciferase for normalization purposes. 7 d after transfection, cells were assayed for firefly and *Renilla* luciferase activities in triplicate per the manufacturer's protocol (Glomax Bioluminescence system; Promega).

Online supplemental material
Table S1 shows the list of PCR primers used for synthesis of dsRNA. Table S2 shows sequences of the oligonucleotides used for EMSA. Online supplemental material is available at http://www.jcb.org/cgi/content/full/jcb.200912024/DC1.

References

Baker, N.E. 2001. Cell proliferation, survival, and death in the *Drosophila* eye. *Semin. Cell Dev. Biol.* 12:499–507. doi:10.1006/scdb.2001.0274

Bhaumik, S.R., and S. Malik. 2008. Diverse regulatory mechanisms of eukaryotic transcriptional activation by the proteasome complex. *Crit. Rev. Biochem. Mol. Biol.* 43:419–433. doi:10.1080/10409230802605914

Brodsky, M.H., W. Nordstrom, G. Tsang, E. Kwan, G.M. Rubin, and J.M. Abrams. 2000. *Drosophila* p53 binds a damage response element at the reaper locus. *Cell.* 101:103–113. doi:10.1016/S0092-8674(00)80627-3

Clemens, J.C., C.A. Worby, N. Simonson-Leff, M. Muda, T. Maehama, B.A. Hemmings, and J.E. Dixon. 2000. Use of double-stranded RNA interference in *Drosophila* cell lines to dissect signal transduction pathways. *Proc. Natl. Acad. Sci. USA.* 97:6499–6503. doi:10.1073/pnas.110149597

de Moor, C.H., H. Meijer, and S. Lissenden. 2005. Mechanisms of translational control by the 3′ UTR in development and differentiation. *Semin. Cell Dev. Biol.* 16:49–58. doi:10.1016/j.semcdb.2004.11.007

de Nooij, J.C., and I.K. Hariharan. 1995. Uncoupling cell fate determination from patterned cell division in the *Drosophila* eye. *Science.* 270:983–985. doi:10.1126/science.270.5238.983

de Nooij, J.C., M.A. Letendre, and I.K. Hariharan. 1996. A cyclin-dependent kinase inhibitor, Dacapo, is necessary for timely exit from the cell cycle during *Drosophila* embryogenesis. *Cell.* 87:1237–1247. doi:10.1016/S0092-8674(00)81819-X

Edgar, B.A., and C.F. Lehner. 1996. Developmental control of cell cycle regulators: a fly's perspective. *Science.* 274:1646–1652. doi:10.1126/science.274.5293.1646

el-Deiry, W.S., S.E. Kern, J.A. Pietenpol, K.W. Kinzler, and B. Vogelstein. 1992. Definition of a consensus binding site for p53. *Nat. Genet.* 1:45–49. doi:10.1038/ng0492-45

el-Deiry, W.S., T. Tokino, V.E. Velculescu, D.B. Levy, R. Parsons, J.M. Trent, D. Lin, W.E. Mercer, K.W. Kinzler, and B. Vogelstein. 1993. WAF1, a potential mediator of p53 tumor suppression. *Cell.* 75:817–825. doi:10.1016/0092-8674(93)90500-P

Farmer, G., J. Bargonetti, H. Zhu, P. Friedman, R. Prywes, and C. Prives. 1992. Wild-type p53 activates transcription in vitro. *Nature.* 358:83–86. doi:10.1038/358083a0

Hershko, A. 2005. The ubiquitin system for protein degradation and some of its roles in the control of the cell division cycle. *Cell Death Differ.* 12:1191–1197. doi:10.1038/sj.cdd.4401702

Hwang, H.C., and B.E. Clurman. 2005. Cyclin E in normal and neoplastic cell cycles. *Oncogene.* 24:2776–2786. doi:10.1038/sj.onc.1208613

Jones, R.G., and C.B. Thompson. 2009. Tumor suppressors and cell metabolism: a recipe for cancer growth. *Genes Dev.* 23:537–548. doi:10.1101/gad.1756509

Kimura, T., M. Gotoh, Y. Nakamura, and H. Arakawa. 2003. hCDC4b, a regulator of cyclin E, as a direct transcriptional target of p53. *Cancer Sci.* 94:431–436. doi:10.1111/j.1349-7006.2003.tb01460.x

Koepp, D.M., L.K. Schaefer, X. Ye, K. Keyomarsi, C. Chu, J.W. Harper, and S.J. Elledge. 2001. Phosphorylation-dependent ubiquitination of cyclin E by the SCFFbw7 ubiquitin ligase. *Science.* 294:173–177. doi:10.1126/science.1065203

Lane, M.E., K. Sauer, K. Wallace, Y.N. Jan, C.F. Lehner, and H. Vaessin. 1996. Dacapo, a cyclin-dependent kinase inhibitor, stops cell proliferation during *Drosophila* development. *Cell.* 87:1225–1235. doi:10.1016/S0092-8674(00)81818-8

Levine, A.J. 1997. p53, the cellular gatekeeper for growth and division. *Cell.* 88:323–331. doi:10.1016/S0092-8674(00)81871-1

Mandal, S., P. Guptan, E. Owusu-Ansah, and U. Banerjee. 2005. Mitochondrial regulation of cell cycle progression during development as revealed by the tenured mutation in *Drosophila*. *Dev. Cell.* 9:843–854. doi:10.1016/j.devcel.2005.11.006

Mao, J.H., J. Perez-Losada, D. Wu, R. Delrosario, R. Tsunematsu, K.I. Nakayama, K. Brown, S. Bryson, and A. Balmain. 2004. Fbxw7/Cdc4 is a p53-dependent, haploinsufficient tumour suppressor gene. *Nature.* 432:775–779. doi:10.1038/nature03155

Matsumoto, A., I. Onoyama, and K.I. Nakayama. 2006. Expression of mouse Fbxw7 isoforms is regulated in a cell cycle- or p53-dependent manner. *Biochem. Biophys. Res. Commun.* 350:114–119. doi:10.1016/j.bbrc.2006.09.003

Minella, A.C., J.E. Grim, M. Welcker, and B.E. Clurman. 2007. p53 and SCFFbw7 cooperatively restrain cyclin E-associated genome instability. *Oncogene.* 26:6948–6953. doi:10.1038/sj.onc.1210518

Mistry, H., B.A. Wilson, I.J. Roberts, C.J. O'Kane, and J.B. Skeath. 2004. Cullin-3 regulates pattern formation, external sensory organ development and cell survival during *Drosophila* development. *Mech. Dev.* 121:1495–1507. doi:10.1016/j.mod.2004.07.007

Moberg, K.H., D.W. Bell, D.C. Wahrer, D.A. Haber, and I.K. Hariharan. 2001. Archipelago regulates cyclin E levels in *Drosophila* and is mutated in human cancer cell lines. *Nature.* 413:311–316. doi:10.1038/35095068

Nagaraj, R., and U. Banerjee. 2004. The little R cell that could. *Int. J. Dev. Biol.* 48:755–760. doi:10.1387/ijdb.041881rn

Nakayama, K.I., and K. Nakayama. 2006. Ubiquitin ligases: cell-cycle control and cancer. *Nat. Rev. Cancer.* 6:369–381. doi:10.1038/nrc1881

Nakayama, K., H. Nagahama, Y.A. Minamishima, M. Matsumoto, I. Nakamichi, K. Kitagawa, M. Shirane, R. Tsunematsu, T. Tsukiyama, N. Ishida, et al. 2000. Targeted disruption of Skp2 results in accumulation of cyclin E and p27(Kip1), polyploidy and centrosome overduplication. *EMBO J.* 19:2069–2081. doi:10.1093/emboj/19.9.2069

Ou, C.Y., Y.F. Lin, Y.J. Chen, and C.T. Chien. 2002. Distinct protein degradation mechanisms mediated by Cul1 and Cul3 controlling Ci stability in *Drosophila* eye development. *Genes Dev.* 16:2403–2414. doi:10.1101/gad.1011402

Owusu-Ansah, E., A. Yavari, S. Mandal, and U. Banerjee. 2008. Distinct mitochondrial retrograde signals control the G1-S cell cycle checkpoint. *Nat. Genet.* 40:356–361. doi:10.1038/ng.2007.50

Perez-Losada, J., J.H. Mao, and A. Balmain. 2005. Control of genomic instability and epithelial tumor development by the p53-Fbxw7/Cdc4 pathway. *Cancer Res.* 65:6488–6492. doi:10.1158/0008-5472.CAN-05-1294

Pickering, B.M., and A.E. Willis. 2005. The implications of structured 5′ untranslated regions on translation and disease. *Semin. Cell Dev. Biol.* 16:39–47. doi:10.1016/j.semcdb.2004.11.006

Reed, S.I. 2003. Ratchets and clocks: the cell cycle, ubiquitylation and protein turnover. *Nat. Rev. Mol. Cell Biol.* 4:855–864. doi:10.1038/nrm1246

Richardson, H., L.V. O'Keefe, T. Marty, and R. Saint. 1995. Ectopic cyclin E expression induces premature entry into S phase and disrupts pattern formation in the *Drosophila* eye imaginal disc. *Development.* 121:3371–3379.

Saville, K.J., and J.M. Belote. 1993. Identification of an essential gene, l(3)73Ai, with a dominant temperature-sensitive lethal allele, encoding a *Drosophila* proteasome subunit. *Proc. Natl. Acad. Sci. USA.* 90:8842–8846. doi:10.1073/pnas.90.19.8842

Singer, J.D., M. Gurian-West, B. Clurman, and J.M. Roberts. 1999. Cullin-3 targets cyclin E for ubiquitination and controls S phase in mammalian cells. *Genes Dev.* 13:2375–2387. doi:10.1101/gad.13.18.2375

Sogame, N., M. Kim, and J.M. Abrams. 2003. *Drosophila* p53 preserves genomic stability by regulating cell death. *Proc. Natl. Acad. Sci. USA.* 100:4696–4701. doi:10.1073/pnas.0736384100

Strohmaier, H., C.H. Spruck, P. Kaiser, K.A. Won, O. Sangfelt, and S.I. Reed. 2001. Human F-box protein hCdc4 targets cyclin E for proteolysis and is mutated in a breast cancer cell line. *Nature.* 413:316–322. doi:10.1038/35095076

Vousden, K.H., and D.P. Lane. 2007. p53 in health and disease. *Nat. Rev. Mol. Cell Biol.* 8:275–283. doi:10.1038/nrm2147

Wimuttisuk, W., and J.D. Singer. 2007. The Cullin3 ubiquitin ligase functions as a Nedd8-bound heterodimer. *Mol. Biol. Cell.* 18:899–909. doi:10.1091/mbc.E06-06-0542

Wolff, T., and D.F. Ready. 1991. The beginning of pattern formation in the *Drosophila* compound eye: the morphogenetic furrow and the second mitotic wave. *Development.* 113:841–850.

Wu, X., J.H. Bayle, D. Olson, and A.J. Levine. 1993. The p53-mdm-2 autoregulatory feedback loop. *Genes Dev.* 7:1126–1132. doi:10.1101/gad.7.7a.1126

Zhang, F., A.J. Paterson, P. Huang, K. Wang, and J.E. Kudlow. 2007. Metabolic control of proteasome function. *Physiology (Bethesda).* 22:373–379.